Kybernetika

Xiangze Lin; Haibo Du; Shihua Li

Parameter influence on passive dynamic walking of a robot with flat feet

Kybernetika, Vol. 49 (2013), No. 5, 792--808

Persistent URL: http://dml.cz/dmlcz/143526

KYBERNETIKA — VOLUME *49* (2013), NUMBER 5, PAGES 792–808

PARAMETER INFLUENCE ON PASSIVE DYNAMIC WALKING OF A ROBOT WITH FLAT FEET

Xiangze Lin, Haibo Du and Shihua Li

The biped robot with flat feet and fixed ankles walking down a slope is a typical impulsive dynamic system. Steady passive gaits for such mechanism can be induced on certain shallow slopes without actuation. The steady gaits can be described by using stable non-smooth limit cycles in phase plane. In this paper, it is shown that the robot gaits are affected by three parameters, namely the ground slope, the length of the foot, and the mass ratio of the robot. As the ground slope is gradually increased, the gaits exhibit universal period doubling bifurcations leading to chaos. Meanwhile, the phenomena of period doubling bifurcations also occur by increasing either the foot length or the mass ratio of the robot. Theory analysis and numerical simulations are given to verify our conclusion.

Keywords: biped robot, impulse dynamic systems, limit cycles, bifurcations, chaos

Classification: 93A14, 93C10,93D15, 93D21

1. INTRODUCTION

Biped robots are typical hybrid dynamic systems [6, 7] and have been studied for well over 30 years. In many areas, biped robots provide potential advantages than wheeled vehicles, such as maintenance of hazardous environments, exploration of unstructured and unpaved terrains, deep-forest logging, fruit harvesting, etc. Therefore, the study of locomotion problem for biped robot is very interesting and has received special attention recently. Among these researches, the analysis of passive walking and design of feedback controllers are two main important issues.

The concept of passive walking for biped robot was first introduced in [17, 18], where a simple biped robot is designed. Under certain initial conditions, the robot can perform a stable passive walking on a range of shallow slopes. After then, the passive walking for biped robot has been further studied by many researchers [1, 2, 3, 4, 5, 10, 13, 19, 27]. In [4, 5], a number of simulation results demonstrated that the biped robot gaits are sensitive to some system parameters, including the ground slope angle, the normalized mass, and the length of the robot. When any of the mentioned three parameters continually changed, the robot gaits exhibited period doubling bifurcations phenomena. In [13, 19], the chaotic gaits for the biped robot were investigated by using the largest Lyapunov exponent and a surrogation analysis method. Based on the theory of hybrid dynamic systems, the stability of the periodic gaits was analyzed in [6, 7].

Another topic in the study of the biped locomotion is how to design feedback controllers. Based on some advanced nonlinear control techniques, many valuable results have been obtained [14 – 23], such as regulation walking on varying slopes [14, 15, 16, 25], regulation walking speed and gait transitions [24], robustness to uncertainties and disturbances [9], etc. In [25], based on passivity mimicking control method, a feedback controller was designed such that the biped robot can perform stable walking on certain steep slopes. In [14, 15], hip joint actuations were used to control bifurcations and chaos in the passive walking. In [16], unstable chaotic gaits were stabilized by using impulsive control and energy shaping method. Robustness issue was discussed by using energy shaping method in [24]. In [9], it was shown that speed regulation and gait transitions can be achieved by using passivity-based control.

However, most of the existing results related to passive dynamic walking are about the biped robot with point or round feet. In order to better imitate human walking, a compass-like biped robot with flat feet and fixed ankles was introduced in [11]. This biped robot with flat feet is not only more like human, but it also has some other advantages. For example, the robot with point feet can not stand alone when it is not walking whereas the robot with flat feet can. However, the authors of reference [11] only investigated that this robot could perform stable passive walking on a range of slopes. If the slope becomes more and more steep, whether the robot gaits are still stable periodic trajectories or exhibit period doubling bifurcations leading to chaos phenomena like the robot with point feet in [4]? On the other hand, the question of how the length of the foot will affect the passive gaits is still unknown. Considering these reasons, it motivates us to analyze the effect of system parameters on gaits of the robot with flat feet. Our contribution in this paper is as follow: 1) The influence of three parameters (i. e., the ground slope, the length of the foot and the mass ratio of the robot) on the robots passive gait are considered. 2) Compared with the case without feet, difference phenomena and advantages of the robot with flat feet were verified.

The rest of this paper is organized as follows. The mathematical model of robot with flat feet is given in Section 2. In section 3, we discuss the existence and stability of limit cycles in passive gaits by using Poincaré map. In section 4, we show that the robot gaits are affected by three parameters, i. e., the ground slope, the length of foot and the mass ratio of the robot. Finally, we come to a conclusion and suggest directions for future research.

2. MATHEMATICAL MODEL

Figure 1 shows the compass-like biped robot with solid flat feet and fixed ankles walking down a slope. The assumptions are listed below as that in [4, 11].

Assumption 2.1.

1. The masses of the robot are concentrated at three points: the hip mass m_H and the leg mass m.

2. The legs are identical: a is the distance between the ankle and the leg mass, b is the distance between the hip and the leg mass, $l = a + b$ is the leg length, c is the distance between the ankle and the end of heel, d is the distance between the

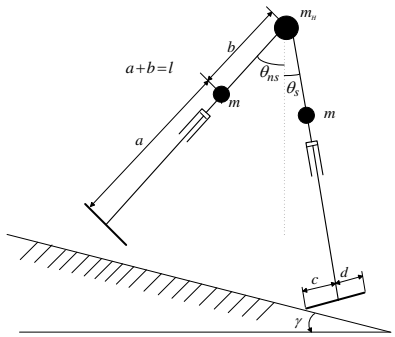

Fig. 1: The robot model with flat feet.

ankle and the end of toe. In addition, the ankle is assumed to fix on the leg and the angle is right angle.

3. There is no actuator in this model.

4. The robot walks down on a plane surface which inclines at a constant angle γ with the horizontal.

5. The robotic knee is prismatic-joint, which is assumed to retract the lower leg to clear the ground. The retraction of the lower leg is massless.

The robot motion consists of two kinds of dynamics, that is swing dynamics and impact dynamics. Next, let us analyze these kinds of dynamics respectively.

1) **Swing stage** (Figure 2(a) and Figure 2(c)). During this stage, one leg is called swing leg which leaves the ground while the other leg supports on the ground and is called support leg. In Figure 2, the angles of the support leg and swing leg relative to the vertical are denoted by θ_s and θ_{ns}. For the plane graph of robot in Figure 2, the positive direction of the each angle is defined as the right angle relative to the vertical and the corresponding angle's value is positive. And the left angle relative to the vertical is the negative direction and its value is negative.

2) **Impact stage** (Figure 2(b) and Figure 2(d)). It occurs instantaneously when the foot of the support leg touches the ground completely or the swing leg hits the ground. Here, as in Ref. [5], the impact leg hitting the ground is assumed to be inelastic and without sliding. So during the instantaneous impact stage, the robot configuration and the total angular momentum are both unchanged, which will lead to a discontinuous change in robot velocity. From a mathematical viewpoint, the impact condition is $\theta_s = -\gamma$ or $\theta_s + \theta_{ns} + 2\gamma = 0$. The detailed derivation for this condition is included in the Appendix.

To analyze the dynamics of the robot motion, one step of the robot motion is divided into four stages in Figure 2, i. e., two swing stages and two impact stages. Each stage has different dynamic equations. The pivot point of the robot is denoted by a black point

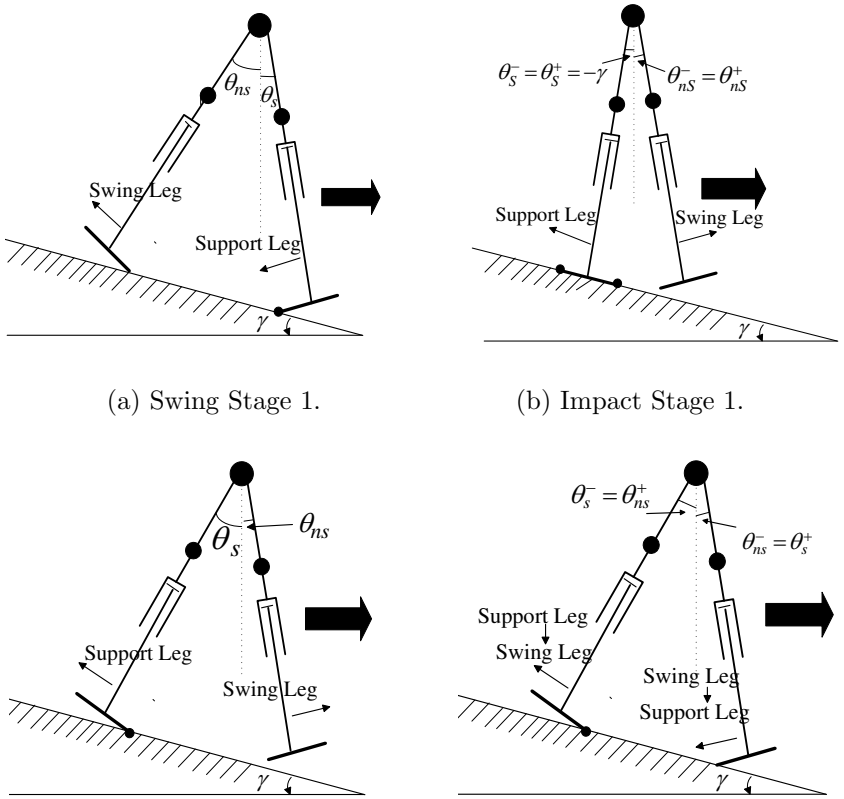

(a) Swing Stage 1. (b) Impact Stage 1.

(c) Swing Stage 2. (d) Impact Stage 2.

Fig. 2: Four dynamic processes of one step motion.

on the foot. The swing direction of the leg is denoted by a arrow. For convenience to understand the motion, the phase plane for one complete step is presented in Figure 3.

Assumption 2.2. During the motion, there is no slipping at the pivot point. The impact is inelastic and without sliding during instantaneous impact stage. This implies that the robot configuration remains unchanged and the angular momentum is conserved.

In the sequel, we will give dynamic equations for each stage. These equations can be found in [11]. We set mass ratio $\mu = m_H/m$ and parameter $c = d$ for this model. The state vector is $x = [\theta_s, \theta_{ns}, \dot{\theta}_s, \dot{\theta}_{ns}]^T \in R^4$. Then the robot system has three variable parameters, i. e., the ground slope γ, the foot length c (or d) and the mass ratio μ.

1) Swing Stage 1 (From Figure 2(a) to Figure 2(b)): In Figure 2(a), the support leg starts to rotate around the end of the heel and the swing leg starts to swing. This is the start of Swing Stage 1. Because that the heel of the supporting leg acts as a pivot

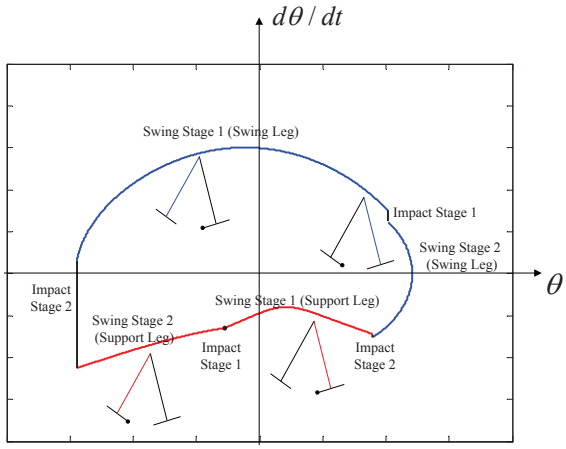

Fig. 3: Phase plane of two (half)-step motion for one leg.

by the assumptions, the dynamic equations of this phase are similar to the equations of a double inverted pendulum. This stage ends when the foot of the support leg touches the ground completely. The dynamic equations are given as:

$$M(\theta)\ddot{\theta} + C(\theta, \dot{\theta})\dot{\theta} + g(\theta) = 0, \tag{1}$$

where $\theta = [\theta_s, \theta_{ns}]^T, \theta_d = \theta_s - \theta_{ns}, g = 9.81m/s^2$,

$$M(\theta) = \begin{pmatrix} \mu(l^2 + c^2) + (l^2 + a^2 + 2c^2) & -b(l\cos\theta_d + c\sin\theta_d) \\ -b(l\cos\theta_d + c\sin\theta_d) & b^2 \end{pmatrix},$$

$$C(\theta, \dot{\theta}) = \begin{pmatrix} 0 & b(c\cos\theta_d - l\sin\theta_d)\dot{\theta}_{ns} \\ -b(c\cos\theta_d - l\sin\theta_d)\dot{\theta}_s & 0 \end{pmatrix},$$

$$g(\theta) = \begin{pmatrix} ((\mu+2)c\cos\theta_s - ((\mu+1)l + a)\sin\theta_s)g \\ gb\sin\theta_{ns} \end{pmatrix}.$$

2) Impact Stage 1 (Figure 2(b)): The Impact Stage 1 occurs when the foot of the support leg touches the ground completely. The angle of the support leg satisfies $\theta_s = -\gamma$. During the impact, the pivot point changes from the heel to the toe of the support leg. The angles θ_s and θ_{ns} keep unchanged while the angular velocities change instantaneously. Since here it is assumed that there is no sliding motion during the impact stage, the heel of stance foot will take off instantaneously after the Impact Stage 1. From Assumption 2.2 and Ref. [11], we obtain the angular velocities satisfy following equations:

$$\theta_s^- = \theta_s^+ = -\gamma, \theta_{ns}^- = \theta_{ns}^+, Q^-(\theta_s^-, \theta_{ns}^-)\dot{\theta}^- = Q^+(\theta_s^+, \theta_{ns}^+)\dot{\theta}^+, \tag{2}$$

where the pre-transition and post-transition variables are identified with the superscripts $-$ and $+$ respectively and

$$Q^-(\theta_s^-, \theta_{ns}^-)$$
$$= \begin{pmatrix} \mu(l^2 - cd) + (l^2 + a^2 - 2cd)) - b(l\cos\theta_d^- + c\sin\theta_d^-) & b(b - l\cos\theta_d^- + c\sin\theta_d^-) \\ -b(l\cos\theta_d^- + c\sin\theta_d^-) & b^2 \end{pmatrix},$$
$$Q^+(\theta_s^+, \theta_{ns}^+)$$
$$= \begin{pmatrix} \mu(l^2 + d^2) + (l^2 + a^2 + 2d^2) - b(l\cos\theta_d^+ - d\sin\theta_d^+) & b(b - l\cos\theta_d^+ + d\sin\theta_d^+) \\ -b(l\cos\theta_d^+ - d\sin\theta_d^+) & b^2 \end{pmatrix},$$

$$\theta_d^- = \theta_s^- - \theta_{ns}^-, \theta_d^+ = \theta_s^+ - \theta_{ns}^+.$$

3) Swing Stage 2 (From Figure 2(b) to Figure 2(c)): This stage starts immediately after the Impact Stage 1 and ends when the heel of the swing leg hits the ground. The dynamic equations are similar to the equations in Swing Stage 1, just replacing c with $-d$ in equation (1). If $c = d = 0$, the dynamic equations in Swing Phase 1 and 2 become the same equations as described in [4, 7, 25] which deal with the compass biped robot with point feet.

4) Impact Stage 2 (Figure 2(d)):The non-supporting leg becomes the supporting leg in this transition. This stage occurs when the heel of the swing leg hits the ground. The impact condition is the angles θ_s and θ_{ns} satisfying $\theta_s + \theta_{ns} + 2\gamma = 0$. After the impact, the swing leg becomes the support leg and vice-versa. At that moment, the angular velocities satisfy following equations:

$$\theta_s^- = \theta_{ns}^+, \theta_{ns}^- = \theta_s^+, Q^-(\theta_s^-, \theta_{ns}^-)\dot{\theta}^- = Q^+(\theta_s^+, \theta_{ns}^+)\dot{\theta}^+, \tag{3}$$

where

$$Q^-(\theta_s^-, \theta_{ns}^-)$$
$$= \begin{pmatrix} -ab + (\mu(l^2 - cd) + 2(al - cd))\cos\theta_d^- - (c + d)(\mu l + l + a)\sin\theta_d^- & -ab \\ -ab & 0 \end{pmatrix},$$
$$Q^+(\theta_s^+, \theta_{ns}^+)$$
$$= \begin{pmatrix} \mu(l^2 + c^2) + (l^2 + a^2 + 2c^2) - b(l\cos\theta_d^+ + c\sin\theta_d^+) & b(b - l\cos\theta_d^+ - c\sin\theta_d^+) \\ -b(l\cos\theta_d^+ + c\sin\theta_d^+) & b^2 \end{pmatrix},$$

$$\theta_d^- = \theta_s^- - \theta_{ns}^-, \theta_d^+ = \theta_s^+ - \theta_{ns}^+.$$

3. A STEADY PASSIVE GAIT

Now, Let us analyze the stability of the robot gaits by using Poincaré map method. In [4], it showed that if the robot can walk down a slope with stable symmetric gaits, it should satisfy: 1)there exists initial condition that leads to a limit cycle in the passive walking; 2)the limit cycle is locally stable.

3.1. Existence of limit cycles in passive gaits

Firstly, let us investigate the existence of limit cycles of the robot with flat feet. We choose the states right after Impact Stage 2 as the Poincaré section Σ. The Poincaré map is illustrated in Figure 4. More details about Poincaré map can be found in [21, 22]. Since the state x has four components, only three components are needed to describe the Poincaré map. Actually, according to the condition for Impact Stage 2, we know that the surface of the Poincaré map is

$$\theta_s + \theta_{ns} + \gamma = 0.$$

Thus the Poincaré map is determined by three variables (i. e. $[\theta_s, \dot{\theta}_s, \dot{\theta}_{ns}]$). But here for the convenience of description of robot walking, we still use $x = [\theta_s, \theta_{ns}, \dot{\theta}_s, \dot{\theta}_{ns}]$.

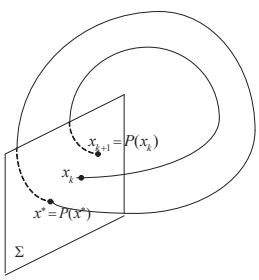

Fig. 4: Poincaré map.

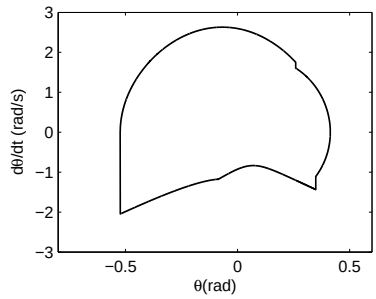

Fig. 5: Period-1 limit cycle.

Definition 3.1. (Parker and Chua [21], Seydel [22]) Let x_k be the kth intersection between the trajectory and the surface of the Poincaré section Σ. The Poincaré map denotes a relation such that

$$x_{k+1} = P(x_k). \tag{4}$$

If this trajectory is periodic through Σ, there is a fixed point x^* that satisfies $x^* = P(x^*)$, which means the system trajectory oscillates around an isolated closed orbit. It is called a limit cycle.

In our model, the parameter values $a = b = 0.5m$, $\mu = 2$, $c = d = 0.1m$, $\gamma = 5^\circ$ are used. Using the algorithm in [21, 22], we find the fixed point is

$$x^* = [0.3487, -0.5231, -1.436, -0.0219]^T.$$

Figure 5 shows the trajectory of one leg of the robot starting from x^*, which is a limit cycle. Note that when the impact occurs, the angular momentum of the robot is conserved during impact. It will lead to a discontinuous change in robot velocity.

3.2. Local stability of limit cycles

Definition 3.2. (Goswami et al. [4]) If any small disturbance is added to a limit cycle, the resulting trajectories converge to the original cycle eventually, then the limit cycle is called locally stable.

For a small perturbation δx^* around the fixed point x^*, the nonlinear mapping function P can be expressed in terms of Taylor series expansion as

$$P(x^* + \delta x^*) \approx P(x^*) + \nabla P(x^*)\delta x^*, \tag{5}$$

where $\nabla P(x^*)$ is a Jacobin matrix of the Poincaré map at the fixed point x^*.

Lemma 3.3. (Seydel [22]) If all eigenvalues of $\nabla P(x^*)$ lie inside the unit circle, then the fixed point x^* of the Poincaré map is locally stable.

Define $\Omega = [\delta x_1^*, \delta x_2^*, \delta x_3^*, \delta x_4^*]$, where $\delta x_1^* = [\varepsilon_1, 0, 0, 0]^T, \ldots, \delta x_4^* = [0, 0, 0, \varepsilon_4]^T$ with ε_i any small scalars, $i = 1, 2, 3, 4$.

Since

$$\nabla P(x^*)\delta x_i^* \approx P(x^* + \delta x_i^*) - P(x^*) = P(x^* + \delta x_i^*) - x^*, \tag{6}$$

then

$$\nabla P(x^*) \approx [P(x^* + \delta x_1^*) - x^*, \ldots, P(x^* + \delta x_4^*) - x^*]\Omega^{-1}. \tag{7}$$

An immediate calculation shows that the eigenvalues of $\nabla P(x^*)$ are

$$[-0.2647 + 0.4388i, -0.2647 - 0.4388i, 0, 0.1562].$$

The corresponding absolute values of these eigenvalues are

$$[0.5125, 0.5125, 0, 0.1562].$$

These values are all less than one, which means that the limit cycle is locally stable.

Remark 3.4. It should be noted that there is a zero eigenvalue for the matrix $\nabla P(x^*)$. Actually, from [20], we know that, if the perturbation is along the limit cycle, the resulting trajectory should be along the same limit cycle, which is the reason for existing a zero eigenvalue. It should be pointed out that this zero eigenvalue is corresponding to the zero Lyapunov's exponent along limit cycle.

In this section, the existence and stability of limit cycles when the robot walks down a shallow slope are verified by numerical simulations. However, when the system parameters (including the slope, the foot length and the mass ratio) vary, a question arises: can the robot still walk down a slope with stable gaits?

4. INFLUENCE OF SYSTEM PARAMETERS ON STEADY PASSIVE GAITS

In the following subsections, we systematically study the effect of the varying system parameters on robot gait by numerical simulations. As mentioned earlier, the system parameters considered are the ground slope γ, the foot length c, and the mass ratio μ. Set $a = b = 0.5m$ for the following analysis.

4.1. Effect of slope

In this subsection, we will investigate the effect of the varying ground slope γ on the robot gait. We set $\mu = 2$ and $c = d = 0.1m$ and increase γ from 0.95° to 7.85° in steps of 0.01°. Figure 6 presents the evolution of the gait step period T as a function of the slope γ. The diagram is called bifurcation diagram [4, 22].

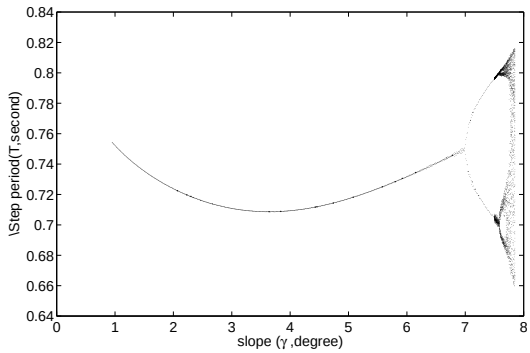

Fig. 6: Bifurcation diagram for step period T as a function of γ.

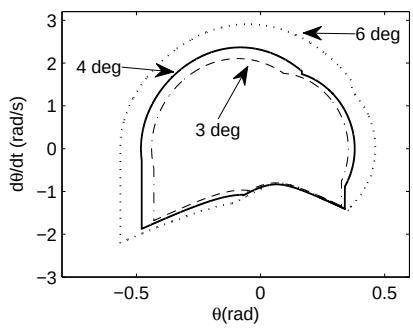

Fig. 7: Phase plane limit cycles for $\gamma = 3°, 4°, 6°$.

From the bifurcation diagram, it can be found that the symmetric gaits are preserved up to $\gamma = 6.73°$. If the ground slope $\gamma < 6.73°$, only one stable limit cycle is found for each γ while the robot takes longer steps as the slope increasing. This behavior can be observed from Figure 7 where the limit cycles are enlarged along both the position and the velocity axes when γ is raised.

The diagram also shows that the first bifurcation occurs at $\gamma = 6.73°$. In fact, at the bifurcation point, one eigenvalue of the Jacobian of the Poincaré map reaches the unit

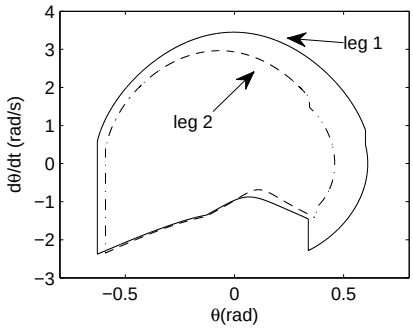

Fig. 8: Period-2 limit cycles at $\gamma = 7.25°$

circle and other eigenvalues stay within the unit circle. By numerical calculation, the eigenvalues of $\nabla P(x^*)$ at $\gamma = 6.73°$ are

$$[-1, -0.2831, 0, 0.0710].$$

After the first bifurcation, the 1-periodic gaits turn into 2-periodic ones. This phenomenon is called period doubling. In this case, the fixed point x^* of the Poincaré map P is replaced by two points with period-2 that are related with

$$x_2^* = P(x_1^*), x_1^* = P(x_2^*).$$

Figure 8 presents limit cycles for 2-periodic gaits at $\gamma = 7.25°$. Each leg now follows a different trajectory, i. e., the robot limps, which implies that the robot gaits become unstable.

Continuously increasing γ, period doubling route to chaos occurs as presented in Figure 6. If the ground slope $\gamma > 7.65°$, the robot gaits become unstable chaotic gaits. Figure 9 shows the phase plane trajectories of the chaotic gaits associated with one leg in 100 steps at $\gamma = 7.75°$.

Remark 4.1. From above analysis, we know that the first bifurcation occurs at $\gamma = 6.73°$. That is to say, the stable symmetric gaits are kept up to $\gamma = 6.73°$. Compared to the robot with point feet in [4], the robot with flat feet can keep stable walking on a larger range of slopes. In [4], it was shown that the first bifurcation of the robot with point feet occurred at $\gamma = 4.37°$ with same fixed system parameters. In addition, it should be pointed out that there is angle less than $6.73°$ for instable cyclic motion. For example, by simulations, we do not observe any stable period-1 limit cycle when the angle $\gamma \leq 0.5°$ under the condition $\mu = 2$ and $c = d = 0.1m$. However, if the foot length and the mass ratio are changed, we can observe stable period-1 limit cycle (e. g., $c = d = 0m$). That is to say, for small slope, the stability depends on the foot length or the mass ratio.

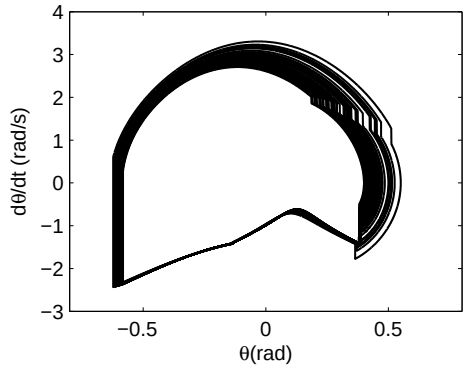

Fig. 9: Phase plane of a chaotic gait associated with one leg.

Remark 4.2. It should be noted that the foot length $c = d = 0.1m$ in all above discussions. In fact, if we set $c = d = 0$, the robot with feet will degenerate into the robot with point feet and the equations in section 2 become the same equations as described in [3, 4, 7], i. e., the robot with point feet is a special case of the one discussed in this paper.

4.2. Effect of foot length

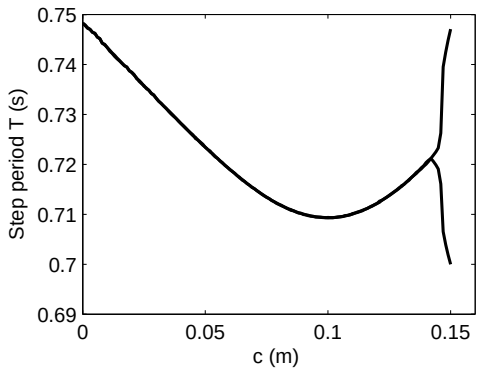

Fig. 10: Bifurcation diagram for step period T as a function of c.

In this subsection, we will discuss the effect of the varying foot length on robot passive gaits. Fixing parameter values $\mu = 2$, $\gamma = 4°$, we increase the foot length c from 0 in steps of $0.001m$ until the robot could not walk. Bifurcation diagram is shown in Figure 10 which presents the evolution of the gait step period T as a function of the foot length c.

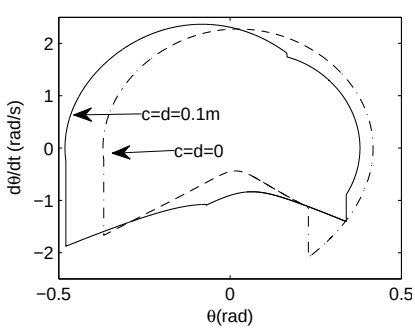

Fig. 11: Phase plane of limit cycles.

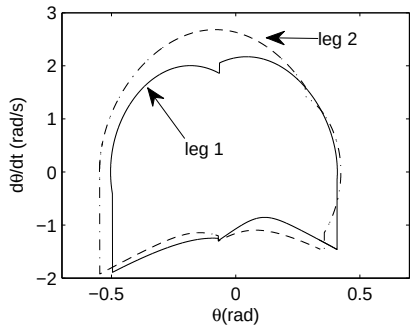

Fig. 12: Phase plane of period-2 limit cycles.

The robot gaits are stable limit cycles for $c < 0.142m$. Two limit cycles corresponding to two different values of foot length $c = 0$ and $c = 0.1m$ are depicted in Figure 11 respectively. It shows that the touchdown inter-leg angle increases for larger c, i. e., the one step length increases. It is obvious that the step period decreases for the robot with feet. This implies that adding feet to a robot increases the walking speed.

From Figure 10, it shows that the robot gaits are 2-periodic for $c \geq 0.142m$. From Figure 12, it shows that period-2 limit cycles at $c = 0.15m$. By continue increasing the foot length from $0.15m$, the robot will not be able to walk down the slope. Note that it is very different from the period doubling route to chaos when the ground slope raised in subsection 4.1.

Remark 4.3. Differing from the robot with point feet, we can regulate the walking speed of the robot with flat feet by choosing different length feet. For example, in the case $\mu = 2, \gamma = 4°$, when the length of foot is 0.1m, the step period T has a minimum.This is a distinct advantage for the robot with flat feet.

4.3. Effect of mass ratio

Without loss of generality, we set $\gamma = 5°$ and $c = 0.1m$. Mass ratio μ is increased from 0.6 to 10 in steps of 0.05. The evolution of the gait step period T as a function of μ is presented in Figure 13. In fact, the robot gaits are still 2-periodic until $\mu \leq 30$.

The robot walking is a stable limit cycle for $\mu < 5.4$. Limit cycles corresponding to different values of μ are depicted in Figure 14. By increasing the parameter μ, we can observe that the step length becomes longer and the step period becomes larger. The period doubling occurs and the robot 1-periodic gaits turn into 2-periodic ones for $\mu \geq 5.4$. Limit cycles for 2-periodic gait at $\mu = 10$ are presented in Figure 15.

In order to compare the influence of mass ration between the biped robot with fixed flat feet and the robot with point feet, we set $\gamma = 4°$ and $c = 0.1m$ since the robot with point feet can not walk on the slope angle $\gamma = 5°$. The evolution of the gait step period T as a function of μ is also given in Figure 16. By a comparison with Fig C12 in Ref. [4],

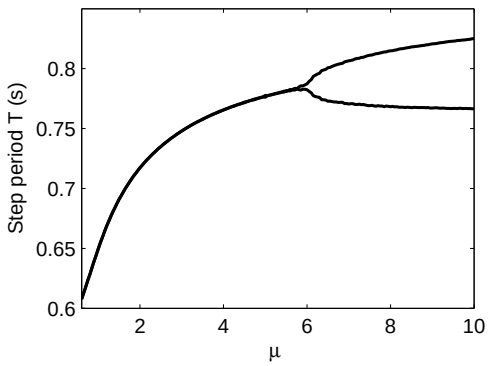

Fig. 13: Bifurcation diagram for step period T as a function of μ.

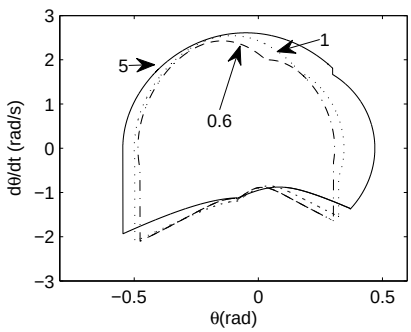

Fig. 14: Phase plane of limit cycles.

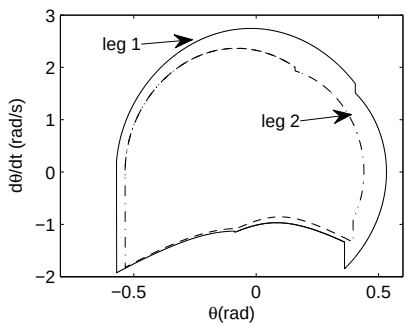

Fig. 15: Phase plane of period-2 limit cycles.

we can find that with the increase of mass ratio, the step period T of biped robot with fixed flat feet is larger than the robot with point feet.

4.4. The two-parameter bifurcation

In this subsection, we will study the analysis of two-parameter bifurcation. Without loss of generality, we set $\mu = 2$. The slope γ is increased from 4° to 5.1° in steps of 0.1° and the foot length c is increased from 0 to 0.15 in steps of 0.015. It can be found that the robot gaits demonstrates bifurcation phenomenon. Figure 17 shows that the length of the foot will affect the first bifurcation point when the ground slope is continuously changed.

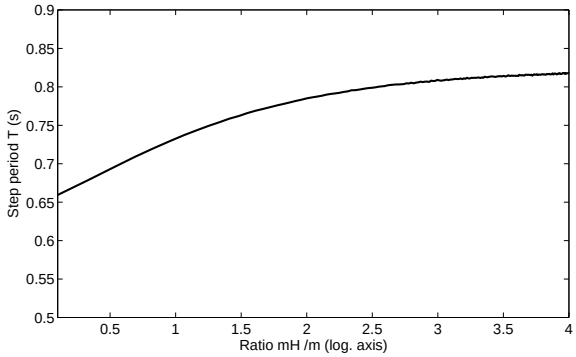

Fig. 16: The evolution of the gait step period T as a function of μ when $\gamma = 4°$.

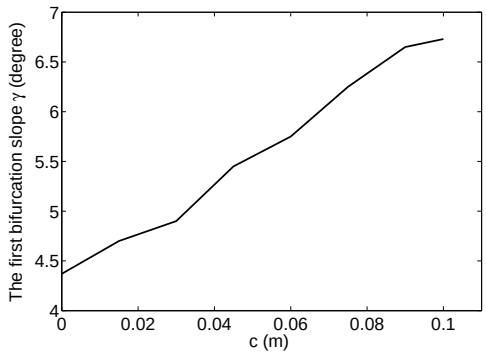

Fig. 17: The influence of the length of the foot on the first bifurcation point.

4.5. Summary of this section

Having discussed the effect of system parameters on the robot with flat feet, now we present some conclusions as follows:

1) According to the previous simulations, we know that if the system parameters chosen appropriately, the robot with feet can keep a stable walking on a certain shallow slope as the robot with point feet. While continuously increasing the slope, period doubling route to chaos occurs. And the phenomenon of period doubling occurs by increasing the foot length and mass ratio, respectively.

2) The robot with point feet is a special case of the one discussed in this paper. Compared to the case without feet, the robot with flat feet can walk a larger range of slopes, which means that adding feet can extend the application range to some extent.

3) With fixed slope and mass ratio, by adjusting the length of foot, the walking speed

of the robot can be regulated.

5. CONCLUSION

The effect of system parameters on passive walking of a robot with flat feet and fixed ankles have been discussed. The robot motion exhibits bifurcation phenomena at a certain slope angle. On further increase in the slope angle, the robot undergoes a period doubling case until its motion becomes chaotic. Bifurcation and period doubling phenomena are also shown to be produced by changing the foot length and the mass ratio. It is interesting to identify the boundary of the basin of attraction with parameter varying where the robot can walk in a steady fashion without any actuation. Also, it deserves to further study how to model the robot with flat feet considering the foot's mass, the reaction forces, and the other configuration of the foot, e. g. compass gait biped with rounded feet or feet with different distance between ankle and heel and ankle and toe, in our future work.

APPENDIX

The appendix collects the detailed derivation of impact condition for Impact Stage 2.

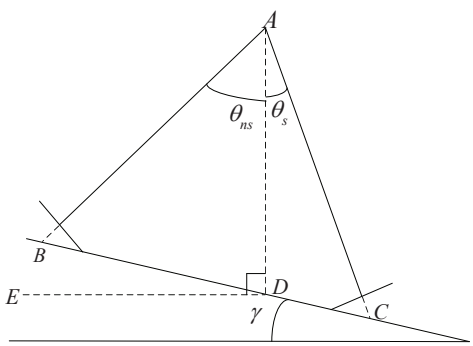

Fig. 18: Geometric pattern for Impact Stage 2.

According to the geometric pattern shown in Figure 18, we know $\angle EDB = \gamma$, which means $\angle ADB = 90^\circ - \gamma$. By the definitions of θ_{ns} and θ_s, and noticing that the superscripts + and − denote the right and left angles relative to the vertical, we obtain

$$\angle ABD = 180^\circ - (90^\circ - \gamma) - (-\theta_{ns}) = 90^\circ + \gamma + \theta_{ns},$$

which leads to $\angle ACD = \angle ABD = 90^\circ + \gamma + \theta_{ns}$. Note that $\angle ADB = \angle ACD + \theta_s$. Then we conclude that

$$\theta_s + \theta_{ns} + 2\gamma = 0.$$

ACKNOWLEDGEMENTS

This work was supported by Natural Science Foundation of China (61074013,61304007), the Program for Postgraduates Research Innovation in University of Jiangsu Province, Youth Sci-Tech Innovation Fund, NJAU (KJ09029), the Fundamental Research Funds for the Central Universities (2012HGBZ0205,2012HGQC0002), China Postdoctoral Science Foundation Funded Project (2012M521217,2013M531372), and Natural Science Foundation of Anhui Province (1308085QF106).

(Received October 9, 2011)

REFERENCES

[1] E. Borzova and Y. Hurmuzlu: Passively walking five-link robot. Automatica *40* (2004), 4, 621–629.

[2] S. Collins, A. Ruina, R. Tedrake, and M. Wisse: Efficient bipedal robots based on passive dynamic walkers. Science *307* (2005), 1082–1085.

[3] M. Garcia, A. Chatterjee, A. Ruina, and M. Coleman: The simplest walking model: Stability, complexity, and scaling. J. Biomech. Engrg. *120* (1998), 2, 281–288.

[4] A. Goswami, B Thuilot, and B. Espiau: Compass-like biped robot Part I: Stability and bifurcation of passive gaits. IINRIA Res. Rep. No. 2996, 1996.

[5] A. Goswami, B. Thuilot, and B. Espiau: A study of the passive gait of a compass-like biped robot: Symmetry and chaos. Internat. J. Robotics Res. *17* (1998), 12, 1282–1301.

[6] J. W. Grizzle, G. Abba, and F. Plestan: Asymptotically stable walking for biped robots: Analysis via systems with impulse effects. IEEE Trans. Automat. Control *46* (2001), 1, 51–64.

[7] I. Hiskens: Stability of hybrid system limit cycles: Application to the compass gait biped robot. In: Proc. IEEE Conference on Decision and Control, Orlando 2001.

[8] J. K. Holm: Control of Passive Dynamic Robots Using Artificial Potential Energy Fields. M. S. Thesis, Univ. Illinois Urbana-Champaign 2005.

[9] J. K. Holm, D. J. Lee, and M. W. Spong: Time scaling for speed regulation in bipedal locomotion. In: Proc. IEEE Conference Robotics Automation, Rome 2007, pp. 3603–3608.

[10] Y. Ikemata, A. Sano, and H. Fusimoto: Analysis of stable limit cycle in passive walking. In: SICE Anual Conference, Fubukui 2003, pp. 117–122.

[11] J. Kim, C. Choi, and M. W. Spong: Passive dynamic walking with symmetric fixed flat feet. In: Proc. IEEE International Conference on Control and Automation, Guangzhou 2007, pp. 24–30.

[12] A. D. Kuo: Stabilization of lateral motion in passive dynamic walking. Internat. J. Robotics Res. *18* (1999), 9, 917–930.

[13] M. J. Kurz, T. N. Judkins, C. Arellano, and M. Scott-Pandorf: A passive dynamic walking robot that has a deterministic nonlinear gait. J. Biomech. *41* (2008), 6, 1310–1316.

[14] M. J. Kurz and N. Stergiou: An artificial neural network that utilizes hip joint actuations to control bifurcations and chaos in a passive dynamic bipedal walking model. Biolog. Cybernet. *93* (2005), 3, 213–221.

[15] M. J. Kurz and N. Stergiou: Hip actuations can be used to control bifurcations and chaos in a passive dynamic walking model. J. Biomech. Engrg. *129* (2007), 2, 216–222.

[16] X. Lin, Y. Ding, M. Shen, and S. Li: Feedback stabilization of unstable periodic orbits for chaotic passive compass-like biped robot. In: Proc. 7th World Congress on Intelligent Control and Automation, Chongqing 2008, pp. 7285–7290.

[17] T. McGeer: Passive dynamic walking. Internat. J. Robotics Res. *9* (1990), 2, 62–68.

[18] T. McGeer: Passive walking with knees. In: Proc. IEEE Conference on Robotics and Automation, Cincinnati 1990, pp. 1640–1645.

[19] D. J. Miller, N. Stergiou, and M. J. Kurz: An improved surrogate method for detecting the presence of chaos in gait. J. Biomech. *39* (2006), 15, 2873–2876.

[20] E. Ott: Chaos in Dynamical Systems. Cambridge University Press, Cambridge 1993.

[21] T. S. Parker and L. O. Chua: Practical Numerical Algorithms for Chaotic Systems. Springer-Verlag, New York 1989.

[22] R. Seydel: Practical Bifurcation and Stability Analysis. Second edition. Springer-Verlag, New York 1994.

[23] M. W. Spong: Passivity based control of the compass gait biped. In: Proc. World Congress of IFAC, Beijing 1999, pp. 19–24.

[24] M. W. Spong and G. Bhatia: Further results on control of the compass gait biped. In: Proc. IEEE International Conference on Intelligent Robots and Systems, Las Vegas 2003, pp. 1933–1938.

[25] M. W. Spong and F. Bullo: Controlled symmetries and passive walking. IEEE Trans. Automat. Control *50* (2005), 7, 1025–1031.

[26] N. Stergiou, U. H. Buzzi, M. J. Kurz, and J. Heidel: Nonlinear tools in human movement. In: Innovative Analysis of Human Movement, Human Kinetics (N. Stergiou, ed.), Champaign 2004.

[27] M. Wisse, A. L. Schwab, and F. C. T. Van der Helm: Passive dynamic walking model with upper body. Robotica *22* (2004), 6, 681–688.

Xiangze Lin, College of Engineering, Nanjing Agricultural University, Nanjing, 210031. P. R. China. (Corresponding author)
e-mail: xzlin@njau.edu.cn

Haibo Du, School of Electrical Engineering and Automation, Hefei University of Technology, Hefei, 230009. P. R. China.
e-mail: haibo.du@hfut.edu.cn

Shihua Li, School of Automation, Southeast University, Nanjing 210096. P. R. China.
e-mail: lsh@seu.edu.cn